APPLIED AND ENVIRONMENTAL MICROBIOLOGY, Oct. 2006, p. 6699–6706 Vol. 72, No. 10
0099-2240/06/$08.00+0 doi:10.1128/AEM.00907-06

Mineralization of Paraoxon and Its Use as a Sole C and P Source by a Rationally Designed Catabolic Pathway in *Pseudomonas putida*

Matthew de la Peña Mattozzi,[1,4] Sundiep K. Tehara,[2] Thomas Hong,[4,5] and Jay D. Keasling[1,2,3,4]*

Graduate Group in Microbiology,[1] Department of Chemical Engineering,[2] Department of Bioengineering,[3] and Department of Molecular and Cell Biology,[5] University of California, Berkeley, California, and Physical Biosciences Division, Lawrence Berkeley National Laboratory, Berkeley, California[4]

Received 20 April 2006/Accepted 4 August 2006

Organophosphate compounds, which are widely used as pesticides and chemical warfare agents, are cholinesterase inhibitors. These synthetic compounds are resistant to natural degradation and threaten the environment. We constructed a strain of *Pseudomonas putida* that can efficiently degrade a model organophosphate, paraoxon, and use it as a carbon, energy, and phosphorus source. This strain was engineered with the *pnp* operon from *Pseudomonas* sp. strain ENV2030, which encodes enzymes that transform *p*-nitrophenol into β-ketoadipate, and with a synthetic operon encoding an organophosphate hydrolase (encoded by *opd*) from *Flavobacterium* sp. strain ATCC 27551, a phosphodiesterase (encoded by *pde*) from *Delftia acidovorans*, and an alkaline phosphatase (encoded by *phoA*) from *Pseudomonas aeruginosa* HN854 under control of a constitutive promoter. The engineered strain can efficiently mineralize up to 1 mM (275 mg/liter) paraoxon within 48 h, using paraoxon as the sole carbon and phosphorus source and an inoculum optical density at 600 nm of 0.03. Because the organism can utilize paraoxon as a sole carbon, energy, and phosphorus source and because one of the intermediates in the pathway (*p*-nitrophenol) is toxic at high concentrations, there is no need for selection pressure to maintain the heterologous pathway.

Organophosphates have been widely used as nerve agents and pesticides. Examples of these compounds include the pesticides coumaphos and parathion and the nerve gas agents soman, sarin, and VX. These compounds irreversibly inhibit acetylcholine degradation in the human body and can kill quickly by causing persistent and uncontrolled muscle stimulation. Parathion, methyl parathion, and paraoxon, three insecticides, are common model organophosphates because they are much less toxic (in rats, the 50% lethal dose of paraoxon is 1.8 mg/kg, compared to 0.001 mg/kg for VX) and less volatile than many nerve agents. Synthetic in origin, many organophosphates are persistent in the environment and resist degradation by naturally extant microorganisms.

Although incineration and chemical hydrolysis have been widely used to destroy these toxic compounds (20), many microorganisms can detoxify organophosphates by hydrolyzing them using organophosphate acid anhydrases. In general, these enzymes have a broad substrate range and can hydrolyze a number of organophosphate contaminants. While one of these enzymes or some variant can allow the initial detoxification of an organophosphate contaminant, the organism may not degrade the hydrolysis products, some of which are toxic and inhibit bacterial growth (13, 33).

The initial hydrolysis of paraoxon by an organophosphate acid anhydrase (Opd from *Flavobacterium* sp. strain ATCC 27551) to *p*-nitrophenol (PNP) and diethyl phosphate (DEP) reduces the toxicity 100-fold. Although it is much less toxic than paraoxon, PNP is still classified as a persistent, priority, toxic contaminant (15, 17, 32). In the environment, PNP is degraded by a few microorganisms, most notably *Moraxella* (30) and *Pseudomonas* isolates (27, 34). The genes responsible for degradation of PNP to β-ketoadipate, which is further converted to acetyl-coenzyme A (acetyl-CoA) and succinyl-CoA, are located in three small operons in a 13.8-kb region cloned from *Pseudomonas* sp. strain ENV 2030 (10, 29, 35).

The other hydrolysis product, DEP, is relatively inert in the environment and has largely been ignored. *Delftia acidovorans*, one of the few organisms known to use DEP as a sole phosphorus source (5, 6), produces a phosphodiesterase (Pde, encoded by the *pde* gene) that hydrolyzes phosphodiester bonds (31). Expression of the gene, with the aid of a native alkaline phosphatase (PhoA from *Pseudomonas aeruginosa* HN854), enabled *Escherichia coli* and the infectious organism *P. aeruginosa* to use DEP as a phosphate source (8, 31).

Though there is no known single microorganism that is capable of hydrolyzing paraoxon and mineralizing its hydrolysis products as a source of carbon and phosphorus, such a strain not only would reduce the toxicity of the organophosphate but also would prevent the accumulation of potentially toxic hydrolysis products in the environment. Furthermore, the engineered strain would be expected to be genetically stable as it would benefit from the genes introduced to mineralize paraoxon. Today we can use the resources of synthetic biology to create a strain that performs catabolic processes that have not been observed in nature. Here we describe the metabolic engineering of a biosafety *Pseudomonas putida* strain to hydrolyze paraoxon and mineralize the hydrolysis products as a source of carbon and phosphorus (Fig. 1). This strain is a prototype for engineered microorganisms capable of consuming any number of organophosphate contaminants and utiliz-

* Corresponding author. Mailing address: Berkeley Center for Synthetic Biology, 717 Potter Street, Building 977, Mail code 3224, University of California, Berkeley, CA 94720-3224. Phone: (510) 495-2620. Fax: (510) 495-2630. E-mail: keasling@berkeley.edu.

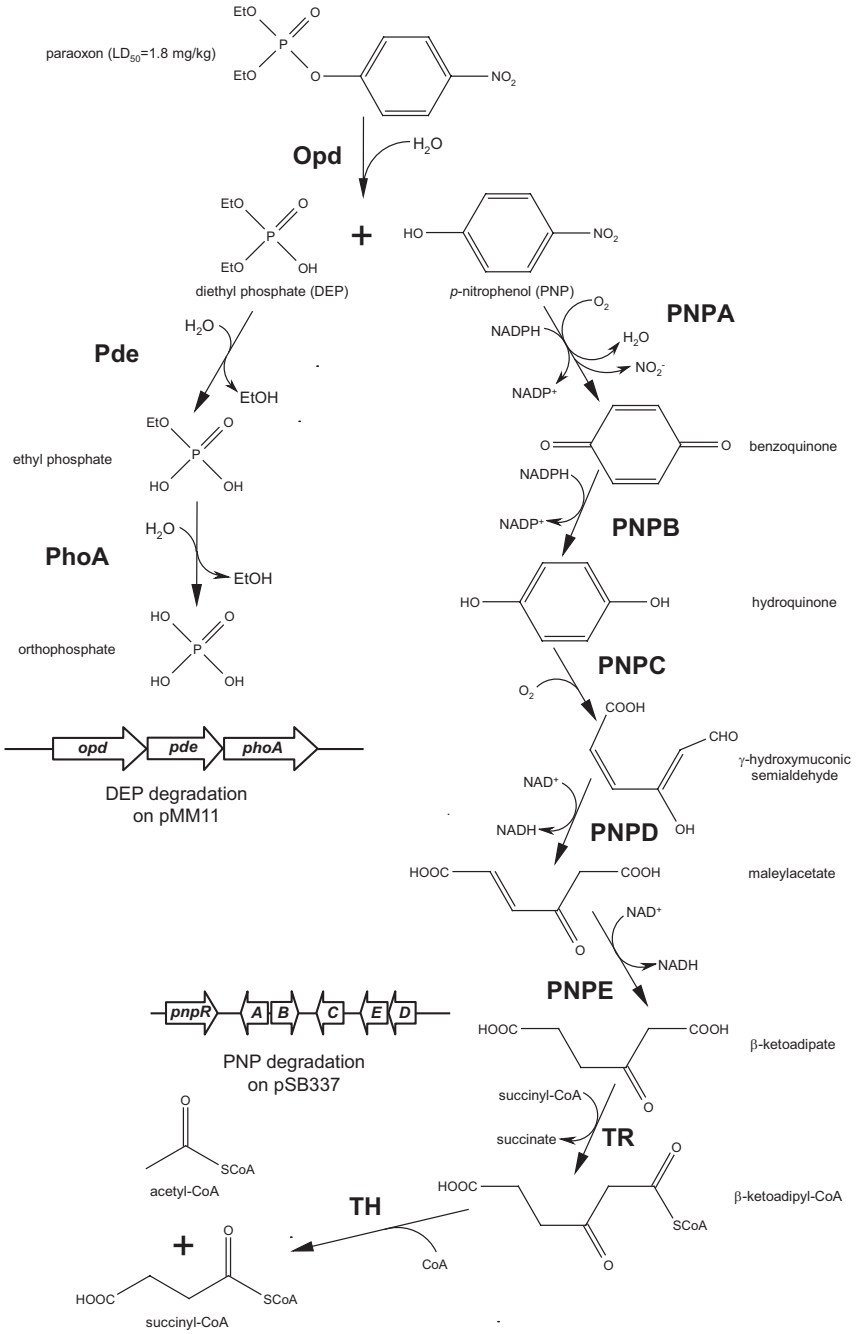

FIG. 1. Engineered biodegradation pathway for paraoxon. Organophosphate hydrolase (Opd) from *Flavobacterium* sp. initially hydrolyzes the pesticide into two primary intermediates, DEP and PNP. DEP is further converted to orthophosphate by a phosphodiesterase (Pde) from *D. acidovorans* and an alkaline phosphatase (PhoA) from *P. aeruginosa*. PNP is converted to β-ketoadipate by five enzymes (encoded by *pnpA* to *pnpE*) from *Pseudomonas* sp. strain ENV2030. β-Ketoadipate enters the tricarboxylic acid cycle as succinyl-CoA and acetyl-CoA after conversion by *P. putida*'s native β-ketoadipate:succinyl-CoA transferase (TR) and β-ketoadipyl-CoA thiolase (TH). LD_{50}, 50% lethal dose.

ing their hydrolysis products for growth, which would be useful for decontamination of equipment contaminated with nerve agents or large-scale destruction of nerve agent stockpiles.

MATERIALS AND METHODS

Strains and media. The strains and plasmids used are listed in Table 1. Luria-Bertani (LB) medium with appropriate antibiotics was used for cloning and in vitro assays. A MOPS (morpholinopropanesulfonate)-buffered minimal medium [40 mM MOPS, 4 mM Tricine, 10 μM $FeSO_4$, 9.5 mM NH_4Cl, 0.5 μM $CaCl_2$, 0.521 mM $MgCl_2$, 50 mM NaCl, 0.276 mM K_2SO_4, 3×10^{-9} M $(NH_4)_6Mo_7O_{24}$, 4×10^{-7} M H_3BO_3, 3×10^{-8} M $CoCl_2$, 1×10^{-8} M $CuSO_4$, 8×10^{-8} M $MnCl_2$, and 1×10^{-8} M $ZnSO_4$, with C and P sources added separately (24)] was used for in vivo assays of paraoxon degradation. This medium allows fine manipulation of phosphate and carbon sources. Paraoxon and diethyl phosphate were obtained from Chem Services, Inc. For solid minimal medium, 2% Noble agar (Difco) was added to the MOPS-buffered minimal medium described above.

Construction of a synthetic operon for paraoxon and DEP hydrolysis. Isolation of the organophosphate hydrolase (*opd*) and phosphodiesterase (*pde*) genes has been described previously (31, 33). Native *opd* was PCR amplified from pWM513 (23) using *Pfu* Turbo polymerase (Stratagene 600256) and primers opdleadfwd (5′-GGA*GGTACC*AGGAGGTTTTTATT**ATG**CAAACGAGAAG GGTTGTGCTCAAGTCTGCGG-3′) and opdrev (5′-TCC*GAATTC*TCATGA

TABLE 1. Strains and plasmids constructed and available in this study

Strain or plasmid	Description	Reference or source
KT2440	Plasmid-cured *P. putida* mt-2	1
HN854	*P. aeruginosa* isolate	H. Nikaido
pSB337	pRK415 containing 12.7-kb region allowing PNP as C source, Tet^r	35
pBBR1MCS2	Broad-host-range plasmid, $LacI^-$, multiple cloning site in LacZ, Kan^r	14
pSTopd3	pBBR1MCS2 with *opd* gene from *Flavobacterium* sp.	This study
pSTopd4	pBBR1MCS2 with *opd* with truncated leader	This study
pSKT11	pBBR1MCS2 with *pde-opd*	This study
pSKT12	pBBR1MCS2 with *pde-opd* with truncated *opd* leader	This study
pBBR2pde	pBBR1MCS2 with *pde* from *D. acidovorans*	This study
pMM05	pBBR1MCS2 with *phoA* from *P. aeruginosa*	This study
pMM06	pBBR1MCS2 with *opd-pde* with truncated *opd* leader	This study
pMM07	pBBR1MCS2 with *opd-pde*	This study
pMM10	pBBR1MCS2 with *opd-pde-phoA* with truncated *opd* leader	This study
pMM11	pBBR1MCS2 with *opd-pde-phoA*	This study

CGCCCGCAAGGTCGGTGACAAGAACCGC-3′) (underlining indicates the ribosome binding site, boldface type indicates the start codon, and italics indicates added KpnI and EcoRI restriction sites in primers opdleadfwd and opdrev, respectively, for cloning into the polylinker in pBBR1MCS2 [14]). The following PCR program was used: 94°C for 1 min, 65°C for 3 min, and 72°C for 2 min for 32 cycles, followed by a 12-min final extension at 72°C. The conserved leader sequence on *opd* was removed by PCR amplifying only the portion of the gene that did not include the N-terminal leader, using *Pfu* Turbo polymerase, primers opdnoleadfwd (5′-GGA*GGTACC*AGGAGGTTTTTATT**ATG**TCGATCGGCA CAGGCGATCGGATCAATAC-3′) and opdrev (see above), and the same PCR program that was used for the native *opd*. The truncated *opd* was present in even-numbered plasmids (Table 1). *pde* was PCR amplified from pTYB1-pdeA (31) using *Pfu* Turbo polymerase and primers pdefwd (5′-GGA*ACTAGT* AGGAGGTTTTTATT**ATG**CACAAGTTCATCCACATCACGG-3′) and pderev (5′-TCC*GAGCTC*CTACGCGCCTAGCCAGAATCTC-3′) (italics indicates added SpeI and SacI restriction sites in primers pdefwd and pderev, respectively, for cloning into the polylinker in pBBR1MCS2). *phoA* from *P. aeruginosa* HN854 was PCR amplified from genomic DNA using *Pfu* Turbo polymerase and primers phoAPfwd (5′-**ATG**ACCCCAGGTTATCCCCTCGCCCTCTCTCTTGCCGTC TCC-3′) and phoAPrev (5′-GTA*GAGCTC*TCAGTCGCGCAGGTTCAGTGC GCGACGG-3′)(italics indicates an added SacI site). A sequence consisting of repeated adenine nucleotides was added to the ends of the PCR product by an additional 12-min extension with *Taq* polymerase. The final PCR product was inserted into a pCR4-TOPO cloning vector (Invitrogen K4580), electroporated into *E. coli* DH10b, and sequenced for directionality. For cloning into pBBR1MCS2, *phoA* was PCR amplified from the TOPO vector using *Pfu* Turbo polymerase, primer phoAPTOPOfwd (5′-GTA*GGATCC*AGGAGGTTTTTAT T**ATG**GCGCGCCAGGACG-3′), and the M13F sequencing primer (5′-GTAA AACGACGGCCAGT-3′) as a reverse primer (italics indicates an added BamHI site). Sequences on all plasmids were confirmed using the UC Berkeley DNA Sequencing Facility.

The PCR-amplified genes were cloned into the polylinker site within the *lacZ* gene on pBBR1MCS2 (14). The host plasmid did not carry a functional *lacI*, so the genes in the operon were constitutively expressed. The organophosphate hydrolase gene (*opd*) was cloned into the vector 5′ of the phosphodiesterase gene (*pde*). The *P. aeruginosa* HN854 alkaline phosphatase gene (*phoA*) was toxic when it was expressed in *E. coli*, so the ligation mixture for any cloning reaction involving expression of this gene was introduced by electroporation into *P. putida* KT2440, bypassing an *E. coli* transformation step. In the final plasmid construct, pMM11, the gene order was *opd-pde-phoA*. Plasmids were transformed into *P. putida* using an established electroporation method (3). The plasmids were maintained by selection on two antibiotics, 5 μg/ml tetracycline for pSB337 and 50 μg/ml kanamycin for pMM11.

Growth assays and real-time determination of *p*-nitrophenol concentrations. Cells were typically grown in MOPS medium with 1 mM succinate or glycerol and 1 mM DEP as C and P sources, respectively, and then inoculated into MOPS medium containing 0.5 or 1 mM paraoxon. Growth assays were typically performed with a 96-well format using a SpectraMax 384 (Molecular Devices, Sunnyvale, CA) or a TECAN SAFIRE (Tecan Ltd., Zurich, Switzerland) to measure optical densities. Cells were grown at 30°C with shaking. Additional assays (Fig. 2) were performed with 50-ml cultures grown in 250-ml baffled Erlenmeyer flasks shaken at 200 rpm at 30°C. Cell densities are reported below as optical densities at 600 nm (OD_{600}).

A method was devised to estimate the real-time concentration of PNP in a 96-well spectrophotometer; this method was modified from a method developed by Miller to measure LacZ activity by the conversion of *o*-nitrophenyl-β-D-galactopyranoside (22). A similar method involves adaptation of Miller's assay for a 96-well plate spectrophotometer (9), but this method allows simultaneous determination of both cell density and PNP concentration. Since cells both scatter and absorb light at all wavelengths, the amount of light absorbed by PNP, which is measured primarily at 402 nm and is used to calculate the concentration of PNP, was corrected for the amount of scattering and light absorbed by the cells at 402 nm. Scattering at 402 nm versus scattering at 600 nm was measured for *P. putida* cells growing in succinate minimal medium (determined empirically at 1.8) and was used to correct the absorbance at 402 nm for PNP (A_{PNP}) in minimal medium containing cells grown on PNP using the formula

$$A_{PNP} = A_{402} - (1.8 \times A_{600})$$

A standard curve for PNP was then constructed for the range of PNP concentrations used in all experiments. The slope (m_{STD}) and intercept (b_{STD}) from this standard curve were used to determine the PNP concentration:

$$[PNP] = (m_{STD} \times A_{PNP}) + b_{STD}$$

Thus, the PNP concentration could be estimated without removing the cells:

$$[PNP] = [m_{STD} \times (A_{402} - 1.8 \times A_{600})] + b_{STD}$$

There was very little scattering due to cell density in the period while PNP accumulated and was degraded. This method gave an estimate of [PNP] and realistic PNP production rates in an experiment.

More precise PNP concentrations were confirmed by repeating the experiments with larger cultures and determining the OD_{600} and [PNP] spectrophotometrically and the [PNP], [DEP], and [paraoxon] by liquid chromatography coupled with triple quadruple mass spectrometry (LC-MS/MS).

In vitro assays of Opd, Pde, and PhoA activities. The cells in 50 ml of a late-exponential-phase (OD_{600}, 0.9) *P. putida* culture grown in LB medium were pelleted and resuspended in 1.5 ml sonication buffer (50 mM Tris, 10% sucrose; pH 8.0). The cells were disrupted by sonication for 2 min. The cell debris was removed by centrifugation, and the lysate was diluted 100-fold in the sonication buffer. The measured activities were normalized to the total soluble protein in each well, which was determined by the bicinchoninic acid assay (Pierce Biosciences, Rockford, Ill.)

(i) Organophosphate hydrolase (Opd) assay. The cell lysate was diluted again fourfold into an Opd assay buffer (100 mM Tris, 1% Triton X-100, 0.8 mM paraoxon; pH 6.92). PNP concentrations were determined colorimetrically at 402 nm against a 0 to 1 mM standard curve at 5-min intervals. The rates of PNP production from paraoxon were calculated and are reported below as the averages of four replicates. Specific activity is reported below in μmol PNP produced h^{-1} mg^{-1} total protein.

(ii) Alkaline phosphatase (PhoA) assay. The cell lysate was diluted fourfold into a PhoA assay medium (750 mM alkaline buffer solution [Aldrich A9226], 0.8 mM *p*-nitrophenyl phosphate; pH 10.3). Specific activity was

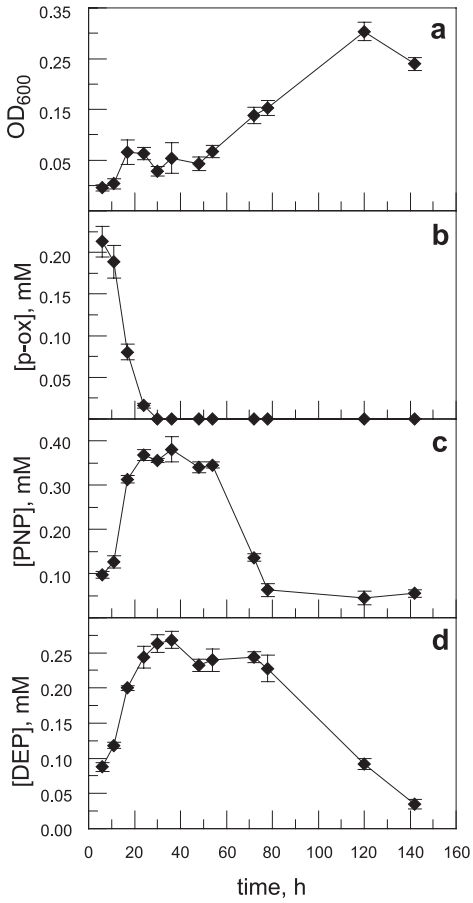

FIG. 2. Degradation of 0.5 mM paraoxon and its use as a sole C and P source. Paraoxon is converted to the intermediates PNP and DEP in the process. The error bars indicate standard deviations for triplicate measurements in a single typical 50-ml culture flask. (a) Optical density. (b) Paraoxon (p-ox) concentration. (c) PNP concentration. (d) DEP concentration.

measured in a fashion similar to the OPD assay, using *p*-nitrophenyl phosphate as an ethyl phosphate analog.

(iii) Phosphodiesterase (Pde) assay. The cell lysate was diluted fourfold into a Pde assay medium (750 mM alkaline buffer solution, 0.8 mM bis-*p*-nitrophenyl phosphate; pH 10.3). Specific activity was measured in a fashion similar to the OPD assay, using bis-*p*-nitrophenyl phosphate as an ethyl phosphate analog. For cells concurrently expressing both *pde* and *phoA*, the PhoA activity was subtracted from the Pde activity, since the product of the Pde reaction is the substrate for the PhoA reaction.

Determination of *p*-nitrophenol, paraoxon, and diethyl phosphate concentrations by LC-MS. The growth of *P. putida* harboring pSB337 and pMM11 in MOPS minimal medium with 0.5 mM paraoxon as the sole carbon and phosphorus source was monitored over a 6-day period. Two novel LC-MS methods were employed to determine paraoxon, DEP, and PNP concentrations in the high-salt MOPS-buffered medium.

(i) Liquid chromatography. An Agilent 1100 high-performance liquid chromatography system (Agilent, Palo Alto, CA) was interfaced with an API 2000 triple quadrupole mass spectrometer (Applied Biosystems, Foster City, CA). Chromatographic separation, where applicable, was performed using a Magic C_{18} column (5 μm; 0.3 by 150 mm; 100 Å RP; Michrom Bioresources, Auburn, CA) at 25°C with a flow rate of 10 μl/min.

(ii) Mass spectrometry. An API 2000 mass spectrometer with an orthogonal electrospray interface (Applied Biosystems, Foster City, CA) was used for all analyses and was operated in MS/MS mode. The drying gas, as well as the nebulizing gas, was nitrogen (Airgas, Berkeley, CA). The source temperature was set to 200°C. The curtain gas flow pressure was set to 20 lb/in^2, and the collision gas flow pressure was set to 2.0 lb/in^2. The ion source gas pressure and turbo spray gas pressure were set to 20 lb/in^2. Infusion experiments were performed using a single syringe pump (Hamilton, Reno, NV) connected directly to the interface. Selected capillary voltages, ionization modes, cone voltages, and collision energies used in multiple reaction monitoring (MRM) mode are shown in Table 2. Dwell times of 500 ms/scan were chosen. Detection and quantification methods were developed and performed using the Analyst software (version 1.4.1; Applied Biosystems, Foster City, CA).

(iii) Quantification of paraoxon using LC-MS/MS. Paraoxon standards at concentrations from 0 to 1 mM were prepared in undiluted MOPS-buffered minimal medium. The samples were diluted 100-fold into 50% methanol–50% water, and 50 μM methionine sulfone was used as an internal standard. A 1-μl portion was applied to the column, using a mobile phase of acetonitrile-water, and the percentage of acetonitrile was changed linearly as follows: 0 min, 20%; 22 min, 50%; 22.1 min, 80%; 33 min, 80%; 33.1 min, 20%; and 40 min, 20%. Paraoxon was detected at 17 min using the positive-mode MRM parameters (Table 2).

(iv) Quantification of PNP and DEP using LC-MS/MS. PNP and DEP standards at concentrations from 0 to 1 mM were prepared combined in undiluted MOPS-buffered minimal medium. The samples were diluted 10-fold into 50% methanol–50% 2 mM tetrabutylammonium acetate (Sigma, St. Louis, MO) with 50 μM methionine sulfone as an internal standard. A 1-μl sample was directly injected through the column into the MS, using a mobile phase of 50% acetonitrile–50% 1 mM tetrabutylammonium acetate and an isocratic method with a 15-min wash. DEP was detected at 2 min and PNP was detected at 3 min using the negative-mode MRM parameters (Table 2).

RESULTS

The primary goal of this study was to engineer an organism that would completely mineralize paraoxon and use it as the sole carbon and phosphorus source for growth. The degradation scheme for accomplishing this goal is shown in Fig. 1. In brief, Opd hydrolyzed paraoxon to DEP and PNP. The PNP was transformed using a known metabolic pathway to β-ketoadipate, which entered the tricarboxylic acid cycle at acetyl-CoA and succinyl-CoA via the action of host-encoded enzymes. The DEP was hydrolyzed using a newly discovered phosphodiesterase (Pde) and alkaline phosphatase (PhoA) to ethanol and orthophosphate, the latter of which could be used as a phosphate source for growth. The enzymes involved in PNP transformation to β-ketoadipate are encoded in a cluster and are from a *Pseudomonas* soil isolate. The genes encoding Opd, Pde, and PhoA were placed in a second operon under the control of a constitutive promoter (*lac* promoter without a *lacI* gene).

TABLE 2. Multiple reaction monitoring parameters for the detection of paraoxon, PNP, and DEP

Compound	Curtain gas pressure (lb/in^2)	Collision-activated dissociation gas pressure (lb/in^2)	Ion spray voltage (V)	Precursor ion (*m*/*z*)	Product ion (*m*/*z*)	Declustering potential (V)	Focusing potential (V)	Entrance potential (V)	Collision cell entrance potential (V)	Collision energy (V)	Collision cell exit potential (V)
Paraoxon	20	20	5,500	276	220	42	400	10	31	27.8	27.0
PNP	10	10	−4,500	138	108	−40	−400	−2	−24.2	−25	−15
DEP	10	10	−4,500	153	79	−40	−400	−2	−22.7	−25	−15

TABLE 3. Opd, Pde, and PhoA specific activities in *P. putida* KT2440 cell lysates

Plasmid	Gene order in operon	Sp act with 0.8 mM substrate (μg PNP produced h^{-1} mg^{-1} protein)			Growth[a]
		Opd	Pde	PhoA	
pMM11	*opd pde phoA*[b]	56 ± 3	6.9 ± 1.1	3.1 ± 0.4	+++
pMM10	*opd pde phoA*	82.4 ± 0.9	1.14 ± 0.17	0.64 ± 0.12	++
pMM07	*opd pde*[b]	35.4 ± 2	1.03 ± 0.18	0.29 ± 0.12[c]	+
pMM06	*opd pde*	43 ± 7	0.5 ± 0.2	0.3 ± 0.2[c]	+
pMM05	*phoA*	0.46 ± 0.20[c]	−0.76 ± 0.12[c]	0.92 ± 0.04	−
pSTopd3	*opd*[b]	8.89 ± 0.61	−0.065 ± 0.046[c]	0.15 ± 0.03[c]	−
pSTopd4	*opd*	24.09 ± 0.43	−0.123 ± 0.177[c]	0.23 ± 0.15[c]	−
pBBR2pde	*pde*	0.48 ± 0.05[c]	2.05 ± 0.34	0.37 ± 0.34[c]	−
pBBR1MCS2	Empty vector	0.14 ± 0.07[c]	0.4 ± 0.3[c]	1.6 ± 1.2[c]	−

[a] Growth with 0.5 mM paraoxon as the sole carbon and phosphorus source, coexpressed with pSB337.
[b] *opd* contained periplasmic leader sequence.
[c] Cells do not express the protein.

Construction of a synthetic operon for paraoxon and DEP hydrolysis. The first step in this work was to design, construct, and optimize an operon to hydrolyze paraoxon and DEP. The optimal gene order for the synthetic operon was determined to be *opd-pde-phoA*, with the native periplasmic leader sequence on *opd*. Paraoxon hydrolysis was not observed in initial studies of any constructs with *pde* expressed 5′ of *opd* (data not shown), so these clones were not pursued further. Assays of enzyme activity for the engineered phosphate utilization pathway showed that the enzymes were active for each of the DEP hydrolysis steps in the host organism, *P. putida* (Table 3).

Interestingly, the putative signal sequence for secretion of Opd into the periplasmic space had an impact on the expression of the other genes in the operon. The specific activity of Opd in constructs carrying the leader sequence at the N terminus of Opd was lower than that in constructs without the leader sequence. Opd specific activity, measured using paraoxon as a substrate, was greatest for cells harboring pMM10 (*opd* without the periplasmic signal sequence, *pde*, and *phoA*) and was ~30% greater than the specific activity for cells harboring pMM11, which expresses *opd*'s native periplasmic signal sequence (Table 3). Thus, cells harboring pMM11 accumulated the toxic intermediate PNP more slowly. Cells harboring the empty vector, pBBR1MCS2, had an Opd specific activity of 0.14 μg PNP produced h^{-1} mg^{-1} total protein, a level that was barely detectable.

In contrast to the impact of the periplasmic leader sequence on Opd, Pde specific activity was higher in strains in which the Opd had a leader sequence than in strains in which the Opd did not have a leader sequence. The Pde specific activity, measured using bis-*p*-nitrophenyl phosphate as a DEP analog, for pMM11-harboring cells was approximately sixfold greater than that for pMM10-harboring cells. The only difference between the two constructs was the periplasmic leader sequence on *opd* in pMM11. The Pde activity from pMM10 and pMM11 was significantly greater than that from all of the other constructs except pBBR2pde (empty vector containing only *pde*). The phosphodiesterase activity in cells harboring the empty vector alone, pBBR1MCS2, was negligible (Table 3).

Similarly, the PhoA specific activity, measured using *p*-nitrophenyl phosphate as an ethyl phosphate substrate analog, was greatest in the strain harboring pMM11 (Opd with leader) and was significantly greater than that for any of the other constructs, including pMM10 (without the *opd* leader sequence) and pMM05 (empty vector containing only *phoA*). The native alkaline phosphatase activity of *P. putida* harboring the empty vector was negligible (Table 3).

It is notable that the specific activities of the enzymes involved in DEP hydrolysis were significantly higher than the specific activity of PnpA, the enzyme responsible for the oxidative denitrification of PNP and the first enzyme in the catabolic pathway. The specific activity of PnpA with 0.8 mM substrate was 0.33 ± 0.05 μg PNP produced h^{-1} mg^{-1} total protein.

Complete mineralization of paraoxon. The engineered operon containing *opd*, *pde*, and *phoA* (pMM11) was transformed into *P. putida* with pSB337, which harbors the *pnp* operon, and paraoxon degradation and growth were monitored in medium in which paraoxon was the sole carbon and phosphorus source. The cultures showed no increase in turbidity for nearly 3 days (Fig. 2a). Nevertheless, the concentration of paraoxon rapidly declined and was undetectable by LC-MS/MS after 24 h (Fig. 2b). The cytotoxic intermediate PNP accumulated in the medium during this time. The average rate of PNP accumulation in the growing cultures was 0.32 mM h^{-1} OD_{600} $unit^{-1}$, and the paraoxon consumption rate was approximately equivalent, 0.36 mM h^{-1} OD_{600} $unit^{-1}$. This PNP accumulation was most apparent in the first 24 h; the PNP concentrations in the flasks remained high until 54 h. The PNP concentrations, measured both optically (Fig. 2c) and using LC-MS/MS (data not shown), reached a maximal level of 0.38 mM during this period. The cells remained in lag phase while the PNP concentration was maximum and entered logarithmic growth after the PNP concentration declined. DEP also accumulated in the medium at this time (Fig. 2d), although the maximum concentration remained 0.25 mM from 24 to 78 h after inoculation. The average rate of DEP accumulation in the medium was 0.28 mM h^{-1} OD_{600} $unit^{-1}$, similar to the rates of paraoxon degradation and PNP production. The DEP concentration remained high until after the cells entered logarithmic growth. Due to matrix effects on MS quantification, the mass balance for the various components (as determined by LC-MS/MS) did not close completely. These effects are discussed below.

Similar results for mineralization of paraoxon were observed in 100-μl cultures assayed in 96-well plates (data not shown). *P.*

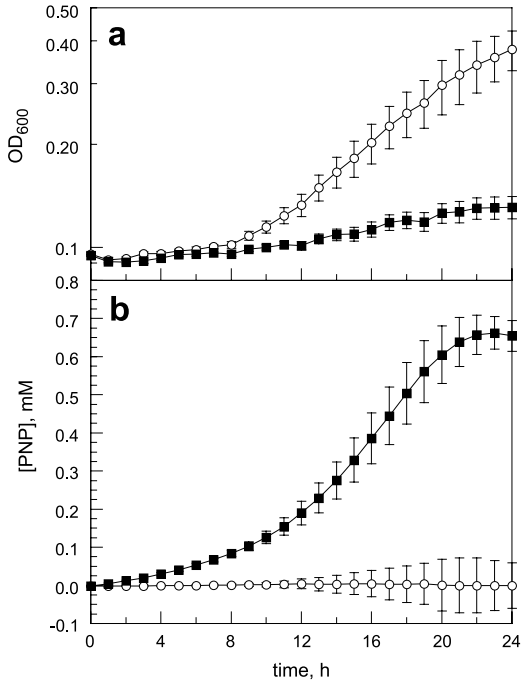

FIG. 3. Production of PNP from paraoxon represses cell growth. *P. putida* harboring either pMM07 (■) or the empty control vector pBBR1MCS2 (○) was grown on a MOPS-buffered minimal medium supplemented with 0.67 mM paraoxon. The error bars indicate standard deviations for four replicate 100-μl cultures. (a) Optical density. (b) PNP concentration.

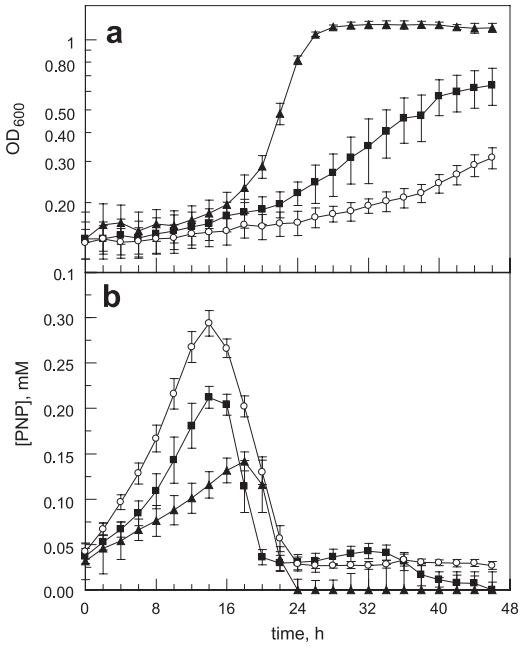

FIG. 4. Growth of and paraoxon degradation by *P. putida* pMM11 pSB337 in the presence of 1 mM DEP or K_2PO_4. The error bars indicate standard deviations for four replicate 100-μl cultures. (a) OD_{600}. (b) PNP concentration. ○, MOPS-buffered minimal medium with 1 mM paraoxon as the sole C and P source; ■, 1 mM DEP added; ▲, 1 mM K_2PO_4 added.

putida mineralized paraoxon up to a concentration of 1.5 mM; higher concentrations resulted in irreversible growth repression by the accumulating PNP. Additionally, when paraoxon was used as a sole carbon and phosphorus source, the cells continued to degrade the pesticide and its hydrolysis products DEP and PNP in the absence of antibiotic selection pressure.

PNP produced from paraoxon represses cell growth. It has been reported that PNP is cytotoxic and represses growth (4, 19). When PNP accumulated in the medium to a high concentration, cell growth, and hence paraoxon degradation, ceased. PNP production was measured optically using a 96-well plate format with cultures of cells expressing *opd* (Fig. 3) in MOPS-buffered minimal medium containing glycerol as a carbon source and supplemented with 1 mM paraoxon. The control culture (harboring the empty vector pBBR1MCS2) did not accumulate PNP and grew to an optical density of 0.5 within 24 h. The cells expressing *opd* accumulated PNP to a concentration of 0.6 mM, and their growth was significantly repressed. PNP accumulation was observed for all strains containing the *opd* gene (data not shown). Addition of pSB337 enabled the cells to use this accumulated PNP as a carbon source.

Growth was phosphate limited. Because *P. putida* does not naturally produce an alkaline phosphatase, it cannot utilize the ethyl phosphate produced from DEP by the action of Pde. When *phoA* from *P. aeruginosa* was expressed in *P. putida*, it was able to use DEP as a sole phosphate source. However, augmentation of the medium with additional, readily usable phosphate sources (e.g., K_2PO_4) reduced the lag time to exponential phase from 40 h to 20 h and the maximal accumulation of PNP from 0.3 mM to 0.15 mM (Fig. 4). A similar result was obtained using DEP as a supplemental phosphate source, but the reductions in lag time and PNP accumulation were less pronounced. In all cases, the PNP degradation appeared to be complete by 20 to 22 h.

DISCUSSION

In this study, we successfully constructed and optimized a novel catabolic pathway for paraoxon and DEP hydrolysis. We introduced this pathway and a second pathway that degrades PNP into the model soil bacterium *P. putida* to enable it to completely mineralize the organophosphate pesticide paraoxon. This rational design of a metabolic pathway for mineralization differs significantly from the traditional bioremediation strategies and represents a new paradigm for laboratory-evolved catabolic pathways (26). One pathway degraded the pesticide into two primary products, DEP and PNP, by the activity of Opd in the synthetic operon. Then, through the activities of Pde and PhoA, the engineered pathway gave *P. putida* the ability to use the DEP as a sole phosphorus source. The other catabolic pathway enabled *P. putida* to use the PNP as a sole carbon and energy source by means of the activities of the five enzymes encoded on pSB337. Paraoxon was completely degraded after 24 h, the PNP was completely consumed after 78 h, and DEP was completely consumed after 142 h. Previous work in our laboratory demonstrated that parathion was used as a carbon source in *P. putida* (33) and in a coculture with *E. coli* (8). In a recent study methyl paraoxon was used as a sole phosphorus source for *E. coli* (21) with a supplemental carbon source. We went a step further and engineered a system to use the organo-

phosphate as a phosphorus source, and we condensed the entire bioremediation system into a single microbe.

Paraoxon hydrolysis and DEP as a sole phosphorus source. *P. putida* KT2440 harboring pMM11 was capable of using paraoxon as a sole phosphorus source. DEP, a nontoxic and relatively inert intermediate, accumulated in the medium (Fig. 2) until the culture reached logarithmic phase and the cell density increased. The cells then used the DEP as their phosphate source after the growth repression due to PNP was overcome (see below). The delay was probably due to the catalytic inefficiency of Pde and PhoA compared to the efficiency of Opd (Table 3). The only genetic difference between pMM11 and pMM10, which had the highest Opd hydrolysis rate, was the periplasmic signal sequence on *opd*. We selected the construct pMM11, which had moderate Opd hydrolysis activity and higher Pde and PhoA hydrolysis activities, to slow production of the intermediates DEP and PNP from paraoxon. This allowed a more optimized DEP production rate and growth.

It is notable that there were polar effects in the synthetic *opd-pde-phoA* operon. Even when Pde and PhoA were expressed alone, the activities of these enzymes were an order of magnitude lower than that of Opd (Table 3). It is also notable that the periplasmic signal sequence on *opd* had polar effects on the expression of the other two genes in the operon; Opd activity was lower when Opd contained a leader sequence, but Pde and PhoA activities were higher. (*phoA* in this synthetic operon contains its native periplasmic signaling sequence, but *pde* is natively expressed in the cytoplasm.) Perhaps increasing the activities by engineering the active sites on the enzymes or the ribosome binding sites in the mRNA transcript may increase their expression and decrease the DEP accumulation.

When paraoxon is used as a sole carbon and phosphorus source, the molar ratio of carbon to phosphorus is 10:1, whereas the molar ratio for the common soil bacterium is closer to 110:1 (4, 19). Despite the excess of phosphorus in paraoxon, this engineered system appeared to be phosphate limited, at least through the initial stages of the degradation process (Fig. 4). The addition of phosphate as K_2PO_4 or DEP increased the growth rate and reduced the concentration of PNP that accumulated in the medium. Addition of K_2PO_4 to the medium increased the growth rate more than addition of DEP increased it; K_2PO_4 was a more readily available phosphate source as it required no enzymatic cleavage for the cells to utilize it. Increased expression of the phosphoesterases may decrease the phosphate limitation in the early stages of growth.

PNP from paraoxon as a sole carbon source. *P. putida* KT2440 expressing pSB337 can use PNP as a sole carbon source, which has been established previously (7, 8, 33, 35). In this case, when *opd* was incorporated into KT2440 harboring pSB337, PNP was generated as paraoxon was hydrolyzed (33). PnpA had a much lower specific activity than Opd, and the resulting accumulation of PNP repressed cellular growth. Degradation of PNP has been identified as a problem previously; various solutions have been devised, such as surface expression of catalytic enzymes (16, 28), increasing inoculum size (34), carbon starvation of the cultures (17), or finding new isolates (15, 18). The concentration of PNP tolerated in this study (up to 0.6 mM) was relatively high compared to concentrations used in these studies, and it was surprising that *P. putida* could tolerate this concentration and still degrade PNP using a natively expressed heterologous system. Regardless, in order for this or any other bioremediation system to be viable, this growth repression has to be overcome. An increased specific activity of PnpA, either due to increased copy number or due to higher catalytic efficiency, will likely decrease the accumulation of PNP.

New, accurate, and rapid detection procedure for paraoxon and DEP. Because of the specific constraints in this study, we developed a novel method to analyze DEP and paraoxon that did not involve derivatization. No offline sample preparation method attempted allowed separation of DEP from the other salts in the MOPS-buffered minimal medium; no offline sample preparation beyond dilution was performed. Most methods for analyzing paraoxon (and the analog parathion) from biological samples using LC-MS depend on fractionation of the paraoxon pesticide into primary breakdown products, including DEP and PNP (2, 25). Since we needed to differentiate between paraoxon and its hydrolysis products, a new method was needed. We developed specialized, differential, LC-MS/MS detection procedures to measure paraoxon in positive-ion mode and DEP and PNP simultaneously in negative-ion mode. The best method previously available (11, 12) did not detect DEP under our LC conditions, so we developed a method that relied on the specific detection abilities of triple quadrupole mass spectrometry rather than separation by high-performance liquid chromatography. Despite the fact that the standards were prepared in the same MOPS-buffered minimal medium in which the cells were grown, matrix effects, caused by components of the cell extract, could not be eliminated. Because of these matrix effects, the mass balance of paraoxon, PNP, and DEP did not close completely. Using LC-MS/MS, the concentration of PNP during the accumulation stage was 0.6 mM and the concentration of paraoxon measured initially was 0.2 mM, despite the fact that the paraoxon concentration in the medium was 0.5 mM before inoculation. To account for this, the PNP values reported above are values from optical measurements. Most importantly, however, the same trends were observed using the two methods: the cells degraded paraoxon to undetectable levels within 24 h, PNP within 78 h, and DEP within 142 h.

In conclusion, in this work *P. putida* KT2440 was engineered with two heterologous pathways which allowed it to completely mineralize paraoxon within 142 h and use it as a sole carbon and phosphorus source. The two significant metabolic bottlenecks—growth repression by the intermediate PNP and phosphate limitation due to low bioavailability of DEP—were both resolved by the time that the pesticide was completely mineralized. Additionally, because the organism can utilize paraoxon as a sole carbon, energy, and phosphorus source and because one of the intermediates in the pathway (*p*-nitrophenol) is toxic at high concentrations, there was no need for selection pressure to maintain the heterologous pathway. Further engineering of the system using paraoxon as a sole C and P source is thus self-optimizing. Future studies to address the viability of this system in an environmental setting (e.g., soil or plant detritus) or in an industrial setting may indicate the power of synthetic biology to produce novel strains for bioremediation. With these studies as a basis, engineering organisms for degradation of other PNP-based organophosphates [parathion,

p-nitrophenylethyl(phenyl)phosphinate, and *O*-ethyl-*O*-4-nitrophenyl phenylphosphonothioate] should be substantially easier and faster. This study demonstrates the potential of using metabolically engineered organisms in remediation processes for organophosphate pesticides and warfare agents.

ACKNOWLEDGMENTS

This research was supported by grants from the National Science Foundation (grant BES-9814088) and the Office of Naval Research (grant N00014-99-1-0182) and by graduate fellowships to S.K.T. from the University of California at Berkeley and the University of California Toxic Substances and Research Teaching Program and to M.D.L.P.M. from the NSF Graduate Research Fellowship Program.

We thank Edward Baidoo and David Garcia for advice in developing LC-MS/MS methods, Gerben Zylstra for the gift of pSB337, Hiroshi Nikaido for the gift of *Pseudomonas aeruginosa* HN854, and Ken Kauffman for useful discussions on metabolism and metabolic modeling.

REFERENCES

1. **Bagdasarian, M., R. Lurz, B. Ruckert, F. C. Franklin, M. M. Bagdasarian, J. Frey, and K. N. Timmis.** 1981. Specific-purpose plasmid cloning vectors. II. Broad host range, high copy number, RSF1010-derived vectors, and a host-vector system for gene cloning in *Pseudomonas*. Gene **16:**237–247.
2. **Cappiello, A., G. Famiglini, P. Palma, and F. Mangani.** 2002. Trace level determination of organophosphorus pesticides in water with the new direct-electron ionization LC/MS interface. Anal. Chem. **74:**3547–3554.
3. **Cho, J.-H., E.-K. Kim, and J.-S. So.** 1995. Improved transformation of *Pseudomonas putida* KT2440 by electroporation. Biotechnol. Tech. **9:**41–44.
4. **Chrzanowski, T., and M. Kyle.** 1996. Ratios of carbon, nitrogen and phosphorus in *Pseudomonas fluorescens* as a model for bacterial element ratios and nutrient regeneration. Aquat. Microb. Ecol. **10:**115–122.
5. **Cook, A. M., C. G. Daughton, and M. Alexander.** 1980. Desulfuration of dialkyl thiophosphoric acids by a pseudomonad. Appl. Environ. Microbiol. **39:**463–465.
6. **Cook, A. M., C. G. Daughton, and M. Alexander.** 1978. Phosphorus-containing pesticide breakdown products—quantitative utilization as phosphorus sources by bacteria. Appl. Environ. Microbiol. **36:**668–672.
7. **Gilbert, E. S., A. W. Walker, S. Davila, and J. D. Keasling.** 2000. Dual species biofilm for bioremediation of the organophosphorus pesticide parathion. Abstr. Pap. Am. Chem. Soc. **219:**U219–U219.
8. **Gilbert, E. S., A. W. Walker, and J. D. Keasling.** 2003. A constructed microbial consortium for biodegradation of the organophosphorus insecticide parathion. Appl. Microbiol. Biotechnol. **61:**77–81.
9. **Griffith, K. L., and R. E. Wolf.** 2002. Measuring beta-galactosidase activity in bacteria: cell growth, permeabilization, and enzyme assays in 96-well arrays. Biochem. Biophys. Res. Commun. **290:**397–402.
10. **Harwood, C. S., and R. E. Parales.** 1996. The beta-ketoadipate pathway and the biology of self-identity. Annu. Rev. Microbiol. **50:**553–590.
11. **Hernandez, F., J. V. Sancho, and O. J. Pozo.** 2002. Direct determination of alkyl phosphates in human urine by liquid chromatography/electrospray tandem mass spectrometry. Rapid Commun. Mass Spectrom.**16:**1766–1773.
12. **Hernandez, F., J. V. Sancho, and O. J. Pozo.** 2004. An estimation of the exposure to organophosphorus pesticides through the simultaneous determination of their main metabolites in urine by liquid chromatography-tandem mass spectrometry. J. Chromatogr. B Anal. Technol. Biomed Life Sci. **808:**229–239.
13. **Hong, F., K. Y. Win, and S. O. Pehkonen.** 2001. Hydrolysis of terbufos using simulated environmental conditions: rates, mechanisms, and product analysis. J. Agric. Food Chem. **49:**5866–5873.
14. **Kovach, M. E., P. H. Elzer, D. S. Hill, G. T. Robertson, M. A. Farris, R. M. Roop, 2nd, and K. M. Peterson.** 1995. Four new derivatives of the broad-host-range cloning vector pBBR1MCS, carrying different antibiotic-resistance cassettes. Gene **166:**175–176.
15. **Kulkarni, M., and A. Chaudhari.** 2006. Biodegradation of *p*-nitrophenol by *P. putida*. Bioresour. Technol. **97:**982–988.
16. **Lei, Y., A. Mulchandani, and W. Chen.** 2005. Improved degradation of organophosphorus nerve agents and *p*-nitrophenol by *Pseudomonas putida* JS444 with surface-expressed organophosphorus hydrolase. Biotechnol. Prog. **21:**678–681.
17. **Leung, K. T., M. Moore, H. Lee, and J. T. Trevors.** 2005. Effect of carbon starvation on *p*-nitrophenol degradation by a *Moraxella* strain in buffer and river water. FEMS Microbiol. Ecol. **51:**237–245.
18. **Leung, K. T., O. Tresse, D. Errampalli, H. Lee, and J. T. Trevors.** 1997. Mineralization of *p*-nitrophenol by pentachlorophenol-degrading *Sphingomonas* spp. FEMS Microbiol. Lett. **155:**107–114.
19. **Makino, W., J. B. Cotner, R. W. Sterner, and J. J. Elser.** 2003. Are bacteria more like plants or animals? Growth rate and resource dependence of bacterial C:N:P stoichiometry. Funct. Ecol. **17:**121–130.
20. **McCloskey, G.** 2001. Johnston Atoll chemical agent disposal system mines its business. Army Chemical Review PB 3-01-02. U.S. Army Chemical School, Fort Leonard Wood, Mo.
21. **McLoughlin, S. Y., C. Jackson, J. W. Liu, and D. L. Ollis.** 2004. Growth of *Escherichia coli* coexpressing phosphotriesterase and glycerophosphodiester phosphodiesterase, using paraoxon as the sole phosphorus source. Appl. Environ. Microbiol. **70:**404–412.
22. **Miller, J. H.** 1992. A short course in bacterial genetics: a laboratory manual and handbook for *Escherichia coli* and related bacteria, 1st ed. Cold Spring Harbor Laboratory Press, Plainview, N.Y.
23. **Mulbry, W. W., and J. S. Karns.** 1989. Parathion hydrolase specified by the *Flavobacterium opd* gene: relationship between the gene and protein. J. Bacteriol. **171:**6740–6746.
24. **Neidhardt, F. C., P. L. Bloch, and D. F. Smith.** 1974. Culture medium for enterobacteria. J. Bacteriol. **119:**736–747.
25. **Olsson, A. O., J. V. Nguyen, M. A. Sadowski, and D. B. Barr.** 2003. A liquid chromatography/electrospray ionization-tandem mass spectrometry method for quantification of specific organophosphorus pesticide biomarkers in human urine. Anal. Bioanal. Chem. **376:**808–815.
26. **Parales, R. E., and J. L. Ditty.** 2005. Laboratory evolution of catabolic enzymes and pathways. Curr. Opin. Biotechnol. **16:**315–325.
27. **Ramanathan, M. P., and D. Lalithakumari.** 1999. Complete mineralization of methylparathion by *Pseudomonas* sp. A3. Appl. Biochem. Biotechnol. **80:**1–12.
28. **Shimazu, M., A. Nguyen, A. Mulchandani, and W. Chen.** 2003. Cell surface display of organophosphorus hydrolase in *Pseudomonas putida* using an ice-nucleation protein anchor. Biotechnol. Prog. **19:**1612–1614.
29. **Spain, J. C.** 1995. Biodegradation of nitroaromatic compounds. Annu. Rev. Microbiol. **49:**523–555.
30. **Spain, J. C., and D. T. Gibson.** 1991. Pathway for biodegradation of *p*-nitrophenol in a *Moraxella* sp. Appl. Environ. Microbiol. **57:**812–819.
31. **Tehara, S. K., and J. D. Keasling.** 2003. Gene cloning, purification, and characterization of a phosphodiesterase from *Delftia acidovorans*. Appl. Environ. Microbiol. **69:**504–508.
32. **United States Environmental Protection Agency.** 2005. National recommended water quality criteria table. United States Environmental Protection Agency, Washington, D.C.
33. **Walker, A. W., and J. D. Keasling.** 2002. Metabolic engineering of *Pseudomonas putida* for the utilization of parathion as a carbon and energy source. Biotechnol. Bioeng. **78:**715–721.
34. **Zaidi, B. R., S. H. Imam, and R. V. Greene.** 1996. Accelerated biodegradation of high and low concentrations of *p*-nitrophenol (PNP) by bacterial inoculation in industrial wastewater: the role of inoculum size on acclimation period. Curr. Microbiol. **33:**292–296.
35. **Zylstra, G. J., et al.** 2000. Microbial degradation of mononitrophenols and mononitrobenzoates, p. 145–160. *In* J. C. Spain, J. B. Hughes, and H.-J. Knackmuss (ed.), Biodegradation of nitroaromatic compounds and explosives. Lewis Publishers, Boca Raton, Fla.